

SOME EFFECTS OF FIELD OF VIEW (FOV) AND TARGET SIZE

ON LATERAL TRACKING AT HOVER

By
Harry T. Breul
Research Department
Grumman Aerospace Corporation
Bethpage, New York

SUMMARY

An exploratory flight-simulator experiment examined the gross effects of several factors potentially important to the design of a visual display system for aiding VTOL pilots in the difficult task of landing on a small sea-control ship. Field of view (FOV) and target size were the primary variables examined for a lateral tracking task in a full motion 5 degree-of-freedom (DOF) hover simulation, mechanized on Grumman's Research Hover Simulator (RHS). Both angular-rate-command and translational-velocity-command control systems were considered as well as two cockpit locations, at the aircraft cg and 15 ft forward of the aircraft cg. Sixteen experimental conditions were examined by two pilots in 105 tracking runs. The mean absolute value (MAV) of tracking error was used to measure tracking performance, and cross spectral transfer function analysis was performed to determine the pilot's ability to generate good open-loop transfer function characteristics as a function of the experimental variables.

In general, it was found that FOV and target size can have a large effect on the pilot's ability to generate open-loop gain, and on his tracking performance.

INTRODUCTION

A crucial element in the success of the sea-control ship concept is the all-weather operations ability of high performance VTOL craft assigned to relatively small ships at sea. The present study was suggested by the following flight scenario:

It's nighttime, there is limited visibility, gusting wind, and a VTOL craft is trying to land on a small pad at the aft end

of a destroyer that is being tossed about by a heavy sea. The darkness and overcast conditions mask any visual information from the pilot's periphery, and the ship's swaying superstructure looms before him to mask any other visual information about his position relative to the "ground". In addition, the cockpit is far in front of the cg, thus exposing the pilot to confounding lateral directional cues while he attempts to track the bounding ship through the narrow aperture of the head-up display (HUD).

The problem, of course, is to define the control and display requirements for safe, effective operation. But first, new data are required to determine things like how to replace the information normally acquired by the pilot in his peripheral FOV, whether he needs that kind of information, or even whether pursuit type information is necessary for tracking the ship's motions, and how a variety of vehicle design and control parameters interact with visual cueing requirements.

The work described here was an exploratory experimental look at the gross effects of two important visual cueing parameters, FOV and target size, and how they affect performance of the kind of lateral tracking required for a landing of VTOL craft on a small sea-control ship. The experiment also included variations in cockpit location and control mode. Two cockpit locations were simulated, at the cg and 15 feet forward of the cg, because many modern VTOL designs place the cockpit well forward. Seated there the pilot might easily confound lateral motion of the cockpit produced by lateral motions of the aircraft with lateral motion of the cockpit produced by aircraft yaw, particularly in conditions of deprived visual cueing. Two aircraft control modes were also simulated: angular-rate command and linear-velocity command. These were chosen to cover the range of candidate control schemes for the next generation of VTOL. The relatively simple-to-mechanize rate-command system requires highly developed piloting skills compared to the more complicated velocity-command system, which even a novice can fly reasonably well.

SYMBOLS

ϕ, θ, ψ	Roll, pitch, and yaw angles about aircraft x, y, and z body axes respectively, DEG.
u, v	Aircraft velocities along the x and y body axes respectively, fps
L_{δ}, M_{δ}	Lateral and longitudinal side-arm controller gains respectively, DEG/SEC ² /DEG
N_{δ}	Rudder-pedal gain, Deg/SEC ² /DEG

X_u, Y_v	Drag terms
$L\dot{\phi}, M\dot{\theta}, N\dot{\psi}$	Angular damping terms, SEC ⁻¹
g	Acceleration due to gravity
\dot{Y}_{GUST}	Inertial reference lateral velocity of aircraft due to atmospheric turbulence, fps
Y_{TAR}	Inertial reference lateral position of target, ft
ϵ	Inertial reference lateral displacement between the target and the simulated aircraft
$\delta_{LAT}, \delta_{LONG}$	Lateral and Longitudinal displacement of side-arm controller, DEG
δ_{RP}	Rudder-pedal deflection, DEG
SUBSCRIPT -	
N	Indicates a sample data quantity, eg $F_N = F(N\Delta t)$

SIMULATION TECHNIQUE

The experiment was performed on Grumman's 6-DOF Research Hover Simulator (RHS) (Fig. 1). Conceptually, the RHS is a continuous-rotation yaw platform, supported by three independently controlled "jacks" mounted on a cart that is driven around the floor by a large "x-y plotter" type mechanism. The three jacks (only two are visible in Fig. 1) impart the pitch, roll, and heave motion to the yaw platform. They are traction-type linear actuators that move up and down a rotating shaft with a speed proportional to shaft rpm. They produce extremely smooth motion with a frequency response that is "flat" out to 4.5 Hz. The other DOF employ more conventional hydraulic drive systems and have frequency responses good to 2-3 Hz.

The hover equations of motion were developed with an eye to simplicity. The experiment was performed in the context of lateral tracking at hover, but the primary variables were visual cueing parameters, rather than subtle variations in dynamic behavior. Thus, no attempt was made to rigorously emulate any particular vehicle dynamics or any particular control system behavior. Also, some simplifying assumptions were made to ease the burden on the small analog computer available for this study. A vector-supported vehicle was assumed with rotational drag about each axis and translational drag along each axis. The only coupling was produced by the horizontal component of the thrust

vector resulting from roll and pitch excursions. Small angle approximations were used. Because of the limited throw of the Z-axis on the RHS (± 1 ft), an aircraft vertical motion was not included, but the cockpit moved vertically due to pitching motions when the simulated cockpit location was forward of the aircraft cg. All control forces were applied as couples. The resulting simplified hover equations of motion for the simulated VTOL vehicle with an angular-rate-command control system are as follows:

$$\dot{u} = g\theta - X_u U \dots\dots\dots 1$$

$$\dot{v} = g\phi - Y_v V \dots\dots\dots 2$$

$$\dot{\phi} = L_\delta \delta_{LAT} - L_\dot{\phi} \dot{\phi} \dots\dots\dots 3$$

$$\dot{\theta} = M_\delta \delta_{LONG} - M_\dot{\theta} \dot{\theta} \dots\dots\dots 4$$

$$\ddot{\psi} = N_\delta \delta_{RP} - N_\dot{\psi} \dot{\psi} \dots\dots\dots 5$$

$$\text{where: } X_u = Y_v = 0.176 \text{ sec}^{-1}$$

$$L_\dot{\phi} = M_\dot{\theta} = 4.587 \text{ sec}^{-1}$$

$$N_\dot{\psi} = 10.00 \text{ sec}^{-1}$$

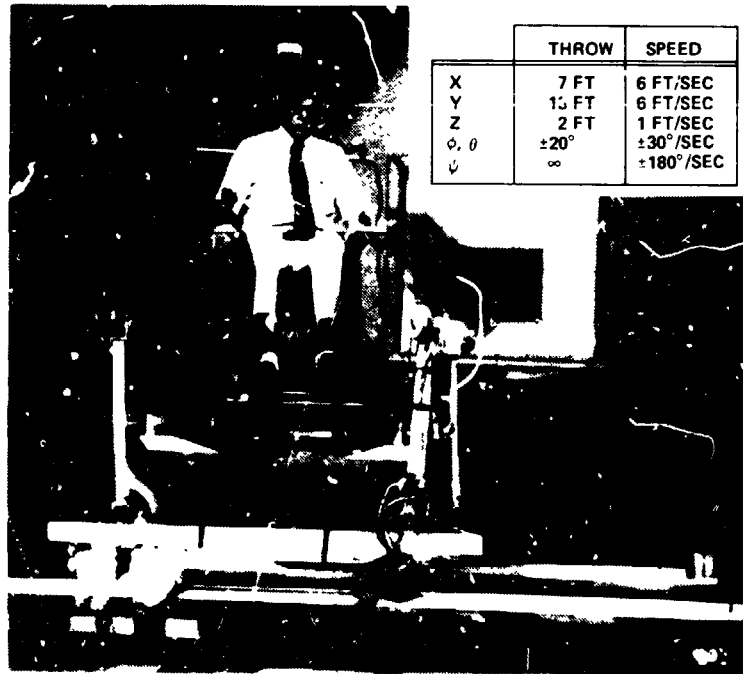
$$L_\delta = 5.64 \text{ deg/sec/deg}$$

$$M_\delta = 7.44 \text{ deg/sec/deg}$$

$$N_\delta = 1.2 \text{ deg/sec/deg}$$

Figure 2 shows the basic computer flow diagram for the v and ϕ DOF. With the function switches open v and ϕ are described by Eq. (2) and (3) for the angular-rate-command control system. The resulting time constants for ϕ and v are 0.22 sec and 5.68 sec respectively. Closing the switches to feedback ϕ and v creates the simple translation-velocity-command control system used in the study ($K_5 = -3.3^\circ/\text{fps}$ and $K_6 = 4.4^\circ/\text{fps}$). The θ , u flow diagram, is nearly identical, increased controller gain being the only difference (K_1 becomes 34 128). The specific values for the coefficients in Eqs (1) thru (5), and the K_5 and K_6 feedback gains, used to produce the translational-velocity-command system, were arrived at empirically. For this purpose we were fortunate to have another large and detailed engineering hover-control simulation being performed at Grumman during the time this study was being formulated. We relied heavily upon comparison with that simulation, both analytically and through a pilot serving both studies, to insure that the simplified equations produced representative dynamics with the two control systems considered.

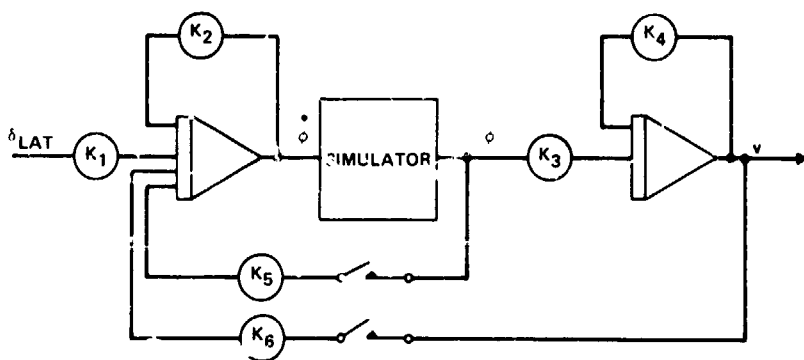
ORIGINAL PAGE IS
OF POOR QUALITY



	THROW	SPEED
X	7 FT	6 FT/SEC
Y	15 FT	6 FT/SEC
Z	2 FT	1 FT/SEC
ϕ, θ	$\pm 20^\circ$	$\pm 30^\circ/\text{SEC}$
ψ	∞	$\pm 180^\circ/\text{SEC}$

0984-0011

Fig. 1 Grumman's Research Hover Simulator (RHS)



0984-002D

Fig. 2 Schematic Computer Flow Diagram for ϕ and v

The pilot made lateral and longitudinal commands with a 2-DOF side-arm controller, and yaw commands with rudder pedals. Both controllers had negligible friction and mild centering forces.

THE EXPERIMENT

Figure 3 presents a composite of the essential elements of the experimental setup used to study how lateral tracking at hover is influenced by two basic elements of the pilot's visual scene: FOV and target size. Two FOV conditions, "wide" ($\pm 105^\circ$) and "narrow" ($\pm 10^\circ$), were studied. They were achieved by adjusting openings in a cockpit hood fitted to the simulator. Two target sizes, "small" and "large", were used to provide two levels of background visibility. The small target was a black vertical rectangle (8 x 30 in) with a 1.0 in. wide white strip down the middle. It was split horizontally, with the bottom half projecting 8.0 in. in front of the top, giving the pilot the parallax between the two pieces as a cue for positioning his craft relative to the target. The background was a white wall with black vertical stripes (16 in. apart) standing immediately behind the target. The photo in Fig. 3 shows the small target against the striped wall. The large target was created by attaching a horizontal 4 x 8 ft sheet of tan foamboard to the rear of the small target. This masked the background wall and simulated the situation in which the pilot's FOV is dominated by the moving superstructure of a ship. Thus, tracking the large target through the narrow opening in the cockpit hood became a pure compensatory task (no background visible), while tracking the small target remained a pursuit task (background visible) for both FOV conditions.

The target moved from side to side in front of the cockpit with a motion like that of the port-to-starboard swaying of a landing platform on the stern of a small destroyer in a heavy sea. This kind of ship motion is characterized as having a lot of energy at a single frequency. Thus the target drive signal was generated by adding the outputs of a sine-wave generator and a pseudorandom noise generator. Tracking runs lasted 204.8 sec and the noise generator created a line spectrum signal with a Δf of 1/204.8 Hz. The single sine wave was at 14/204.8 Hz, and the two signal generators were synchronized so that the target motion time-history was repeated identically every 204.8 sec. The envelope of the amplitude spectrum of target motion is shown in Fig. 4.

The detailed engineering hover simulation mentioned in the previous section was used to generate simplified gust disturbance data for use with the simplified vehicle simulation. The engineering simulation model was excited by a Dryden model (Ref 1) of atmospheric turbulence (RMS velocity = 4 fps) having a mean wind direction perpendicular to the nominal longitudinal plane. The resulting aircraft lateral inertial velocity was recorded and used as a gust-like disturbance in the present work by adding

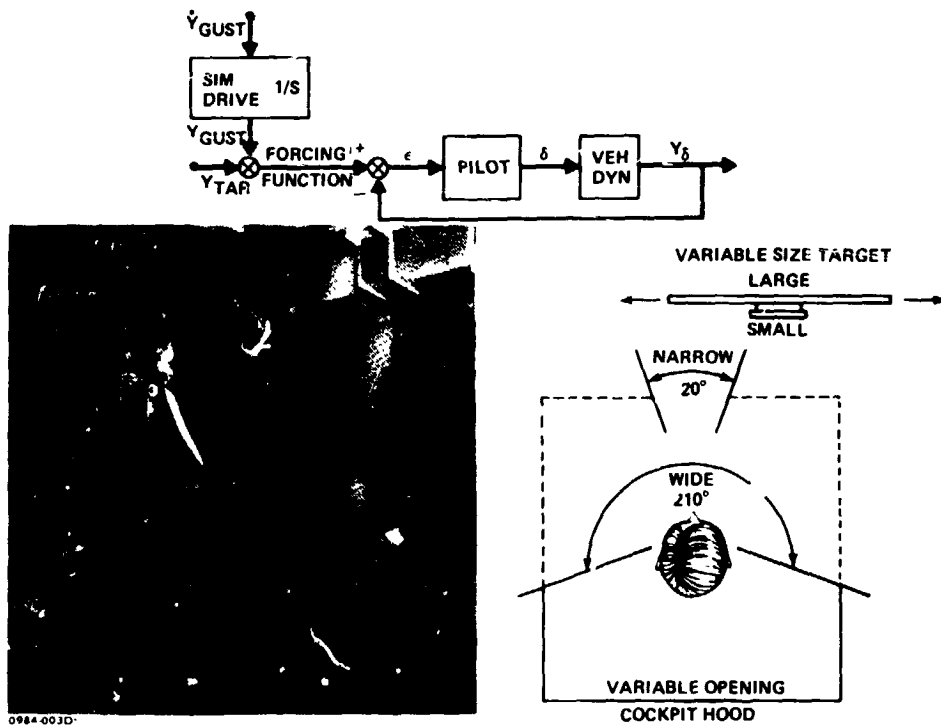


Fig. 3 Experimental Setup

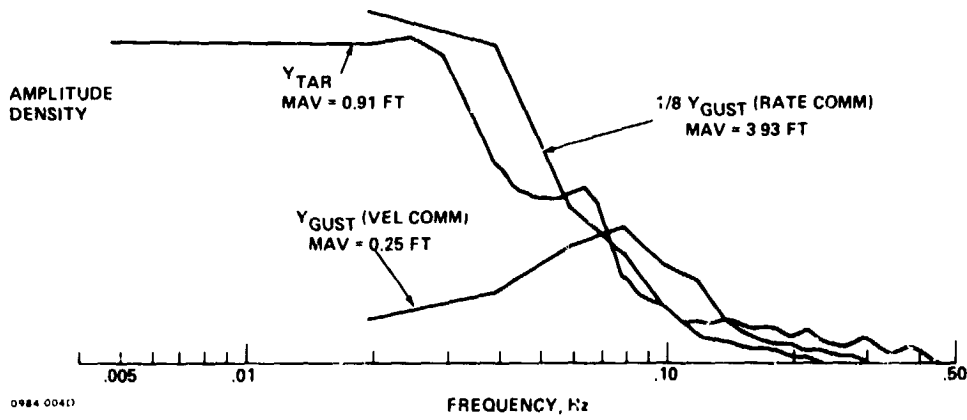


Fig. 4 Amplitude Spectra of Target and Gust Disturbances

it to the simulated aircraft's lateral inertial velocity. The amplitude spectra of the resulting gust disturbances created for use with the angular-rate and translational-velocity control systems are shown in Fig. 4. The velocity-stabilizing feature of the translational-velocity control system acts as a strong gust suppressant and dramatically changes the character of the tracking task for the two control systems. In addition to the primary disturbances described in Fig. 4, a small low frequency disturbance was also introduced in yaw (std dev = 7.1°/sec) to insure that the pilot would have to exercise the yaw DOF. With the very simple equations of motion used, no yaw motion would otherwise occur.

Sixteen experimental conditions are created by considering all combinations of the two levels of the four variables: FOV (wide and narrow), target size (large and small), control mode (angular-rate-command and translational-velocity-command), and cockpit location (at the cg and 15 ft forward of the cg). Two pilots made a total of 105 tracking runs at the 16 experimental conditions, and the order of presentation was randomized. One pilot was a recently retired (6 mos) Navy pilot with 800 hr fixed wing experience and 3700 hr in rotary wing craft, one-third of that gained operating off a ship at sea. The other "pilot" was a simulator engineer with over 20 years experience flying research and engineering simulations.

DATA AND ANALYSIS

During each 204.8 sec tracking run five variables were sampled at the rate of 10 samples/sec and stored on magnetic disc. They were: target position, Y_{tar} , tracking error, ϵ , lateral velocity due to gust, \dot{Y}_{gust} ; lateral controller position, δ_{lat} ; and yaw angle, ψ . The MAV and amplitude spectra of ϵ were calculated for all runs by both pilots. Pilot/vehicle open-loop transfer functions were also calculated, but for the helicopter pilot only. To do this, a sample data time history of aircraft lateral displacement due to pilot control, Y_{δ} (see Fig. 3), was needed. It was computed from the stored data as follows:

$$(Y_{\delta})_N = (Y_{tar})_N + (Y_{gust})_N - \epsilon_N$$

where $(Y_{gust})_N$ was created by numerically integrating $(\dot{Y}_{gust})_N$. The process left a constant of integration unaccounted for, and the mean value of $(Y_{\delta})_N$ in error. This was acceptable, however, because the harmonic analysis normalized the raw data by removing the mean.

DISCUSSION OF RESULTS

In this exploratory study, gross effects on performance were being examined, and the MAV of tracking error was the measure of performance used to compare the effects of the experimental variables. The averages of MAV tracking error for both pilots at each condition are summarized in Fig. 5. The "t" test (Ref 2), for measuring the confidence of differences between means, was applied to the data. MAV's significantly different (at the 5% level) are joined by brackets in the margin. Significant differences due to a single variable are indicated by brackets in the right hand margin and important significant differences due to more than one variable are indicated by brackets in the left hand margin. No comparisons were made between the angular-rate-command and the translational-velocity-command configurations. The shaded test conditions (4, 8, 12 and 16) all have the combination of narrow FOV and large target size. This results in completely masking all background information from the pilot's view, and changes the task from pursuit to compensatory tracking. These configurations produced an extreme degradation of visual cueing and are valuable as a sort of "benchmark", but, because they also produced a discrete change in task, they were not used for direct evaluation of the experimental variables. Therefore, significant variations involving the shaded configurations are not indicated in the figure.

CONTROL MODE	TEST CONDITION		MAV OF ϵ , IN.	NO. OF TRIALS	STD DEV
	NO.	CONFIG*			
RATE COMMAND	1	WSA	6.9	4	0.42
	2	NSA	8.3	7	0.64
	3	WLA	7.7	9	0.51
	4	NLA	8.7	8	0.70
	5	WSF	7.8	7	0.64
	6	NSF	7.7	4	0.67
	7	WLF	7.9	6	0.67
	8	NLF	8.2	5	0.78
VELOCITY COMMAND	9	WSA	4.5	4	0.44
	10	NSA	4.7	10	0.24
	11	WLA	4.9	10	0.47
	12	NLA	4.2	3	0.38
	13	WSF	4.8	7	0.42
	14	NSF	4.7	7	0.31
	15	WLF	5.3	7	0.53
	16	NLF	4.8	7	0.30
COMPENSATORY TRACKING		*CONFIG LEGEND			
		 — Cockpit Location: At cg or 15 ft Fwd — Target Size: Large or Small — Field of View: Wide or Narrow			

Fig. 5 Mean Absolute Value (MAV) of Tracking Error ϵ

For angular-rate-command control systems condition 1 is baseline (wide FOV, small target and cockpit at the cg). The best rate-command tracking performance is achieved at this condition. Comparison with condition 2 reveals a strong significant change in tracking performance due to reduced FOV. We hypothesize that it is a deterioration of inner-loop roll control due to a loss of roll-rate information from the pilot's peripheral FOV that leads to the poorer lateral tracking at condition 2. Roll and roll-rate information are still available in the pilot's foveal FOV because the striped wall is still visible behind the small target through the narrow opening. However, the loss of cues from the pilot's periphery is apparently crucial. Comparison of condition 1 with condition 3 shows that masking the background in the pilot's foveal FOV with the large target also produces a significant deterioration in tracking performance at condition 3. Here the pilot's peripheral information is not degraded and we suggest that neither are roll stabilization and control. Instead, we hypothesize that the lateral tracking suffers directly from the pilot's loss of information about the lateral motion in the outer-loop tracking task itself. That is, the edges of the large target are outside the pilot's foveal FOV and this reduces the precision with which he can visually sense pursuit-type information about target motion against the wall. Because tracking performance at condition 3 is also significantly different from tracking performance at condition 2 we can conclude that FOV has a stronger effect than target size.

The effect of moving the cockpit forward of the cg does not appear totally consistent. It clearly reduces tracking performance for the baseline configuration (condition 5 vs condition 1), but the combined effects of cockpit location and FOV (condition 6 vs condition 2) or cockpit location target size (condition 7 vs condition 3) are no greater than either effect alone.

In general, tracking error at the velocity-command conditions is much less than at the rate-command conditions, but it is not significant because the total forcing function (Fig. 3) was greatly reduced. This resulted from simulating the gust alleviation effect that is characteristic of velocity-stabilizing control systems by using a lateral inertial disturbance with much less energy (Fig. 4). What is of interest is the sensitivity of tracking performance with the velocity-command system to the experimental variables. For the translational-velocity-command control systems, condition 9 is the baseline (wide FOV, small target and cockpit at the cg). The first and obvious result is that neither reduced FOV nor increased target size significantly diminished tracking performance from the baseline (condition 9 vs conditions 10 and 11). If we believe, as suggested earlier, that FOV affects inner-loop roll stabilization, then we would not expect FOV to have an effect with the velocity-command control system, where the pilot is relieved of roll control. We would still expect target size to produce an effect on tracking performance, and suggest that the task has become so much easier (with velocity-command and the greatly reduced gust disturbance) that the effect is not critical (condition 9 vs condition 11). In this regard the effect of cockpit location is very interesting. The lateral tracking task

becomes more difficult when the cockpit is 15 ft ahead of the cg and the pilot must differentiate between lateral motion of the cockpit due to lateral motion of the aircraft and lateral motion of the cockpit due to yaw. This increased difficulty due to cockpit location does result in poorer tracking performance but only with the large target (condition 11 vs condition 15). Also, this relatively poor tracking is improved when reverting to the small target with either FOV (condition 15 vs condition 14 or 13). Thus, we conclude that FOV does not affect tracking with the roll-stabilized-velocity command system and that target size does, at least at the more difficult forward location of the cockpit. This is consistent with the effects observed with the rate-command system and supports the notion that peripheral FOV information is needed for inner-loop roll stabilization and that foveal FOV information is needed for the outer-loop position tracking.

A limited amount of harmonic analysis was performed on some of the time-history data. Figure 6 is a plot of the amplitude spectral density of tracking error achieved at rate-command test conditions 1, 2 and 3 by the subject who is an experienced helicopter pilot. The curves are averages of from 3 to 6 repeats. The standard deviation shown is an aggregate for all curves. Test conditions 1, 2 and 3 demonstrate most dramatically the effects of FOV and target size. The plot shows a fairly uniform increase over the range of input frequencies (see Fig. 4) due to

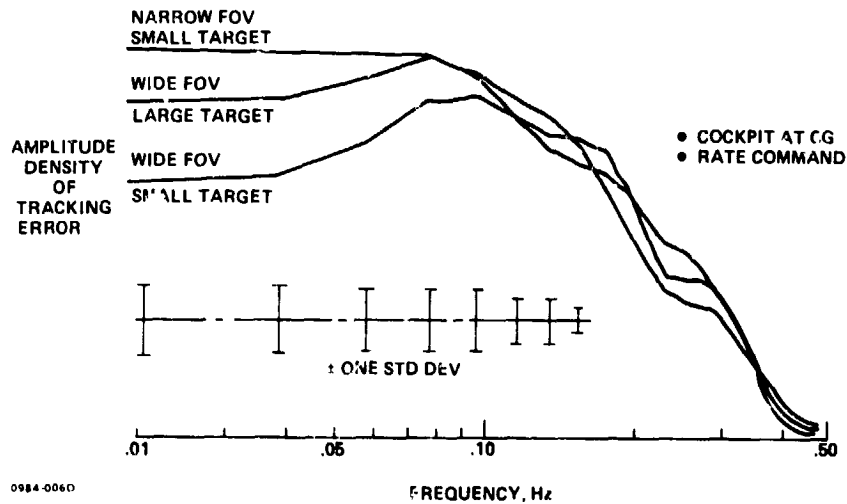


Fig. 6 Tracking Performance for Three Viewing Conditions

both decreased FOV and increased target size. Figure 7 is a plot of open-loop gain (see Fig. 3) for the same three conditions by the same subject. There was no variation in phase margin and the single plot shown is typical. The data indicate that the principle effect of both FOV and target size was to reduce the outer-loop position tracking, open-loop gain. We have indicated that the tracking error data suggest that FOV and target size affect different parts of the pilot's control activity. These curves show that the end result is to simply alter the open-loop gain.

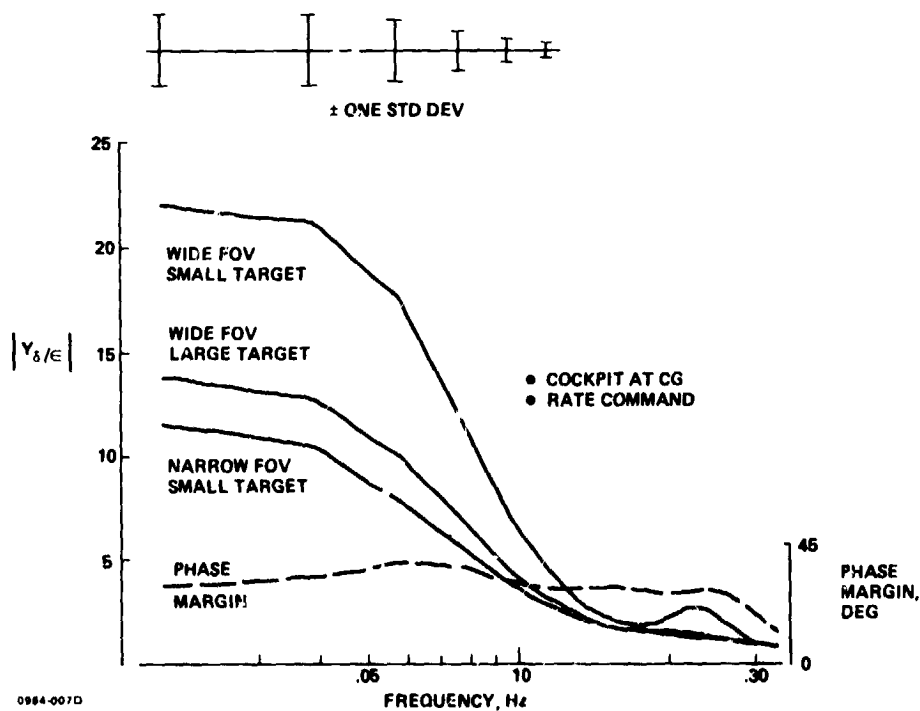


Fig. 7 Open-Loop Gain for Three Viewing Conditions

CONCLUDING REMARKS

An exploratory, full motion, 5-DOF simulator experiment using simplified dynamics has shown that FOV, target size, and cockpit location have a significant effect on a pilot's ability to perform lateral tracking at hover. Tracking error data support the hypothesis that the effects of FOV are largely separable from the effects of target size, FOV affecting inner-loop roll control, and target size affecting outer-loop tracking performance directly. Transfer function analysis suggests that both target size and FOV ultimately affect the outer-loop tracking performance by changing the outer-loop, open-loop gain the pilot can generate.

In a practical sense the results suggest that to achieve good lateral tracking performance at hover a pilot needs to sense roll information in his peripheral FOV or have the roll DOF stabilized. Normal roll information in the pilot's foveal FOV does not suffice. The results also show that added cockpit motion due to yawing about a cg aft of the cockpit can be detrimental, particularly when tracking large objects at close range, and suggests that the yaw DOF be stabilized for performance of analogous flight tasks.

REFERENCES

1. Chalk, C.R., et al: Background Information and User Guide for MIL-F-8785B (ASG), Military Specification - Flying Qualities of Piloted Airplanes. Air Force Flight Dynamic Laboratory Technical Report AFFDL-TR-69-72, Air Force Systems Command, Wright-Patterson Air Force Base, Ohio, August 1969.
2. Hoel, Paul G.: Introduction to Mathematical Statistics, John Wiley & Sons. New York, 1947.